

UAV-Assisted Space-Air-Ground Integrated Networks: A Technical Review of Recent Learning Algorithms

Atefeh Hajijamali Arani, Peng Hu, *Senior Member, IEEE*, and Yeying Zhu, *Member, IEEE*

Abstract—Recent technological advancements in space, air and ground components have made possible a new network paradigm called “space-air-ground integrated network” (SAGIN). Unmanned aerial vehicles (UAVs) play a key role in SAGINs. However, due to UAVs’ high dynamics and complexity, the real-world deployment of a SAGIN becomes a major barrier for realizing such SAGINs. Compared to the space and terrestrial components, UAVs are expected to meet performance requirements with high flexibility and dynamics using limited resources. Therefore, employing UAVs in various usage scenarios requires well-designed planning in algorithmic approaches. In this paper, we provide a comprehensive review of recent learning-based algorithmic approaches. We consider possible reward functions and discuss the state-of-the-art algorithms for optimizing the reward functions, including Q-learning, deep Q-learning, multi-armed bandit (MAB), particle swarm optimization (PSO) and satisfaction-based learning algorithms. Unlike other survey papers, we focus on the methodological perspective of the optimization problem, which can be applicable to various UAV-assisted missions on a SAGIN using these algorithms. We simulate users and environments according to real-world scenarios and compare the learning-based and PSO-based methods in terms of throughput, load, fairness, computation time, etc. We also implement and evaluate the 2-dimensional (2D) and 3-dimensional (3D) variations of these algorithms to reflect different deployment cases. Our simulation suggests that the 3D satisfaction-based learning algorithm outperforms the other approaches for various metrics in most cases. We discuss some open challenges at the end and our findings aim to provide design guidelines for algorithm selections while optimizing the deployment of UAV-assisted SAGINs.

Index Terms—Unmanned aerial vehicles, satellite networks, terrestrial networks, deployment, reinforcement learning, heuristic algorithms

I. INTRODUCTION

THE recent advancements in the non-geostationary-orbit (NGSO) satellite networks, aerial and terrestrial networks have enabled the new paradigm called “space-air-ground integrated networks” (SAGINs). Unmanned aerial vehicles (UAVs) are an essential part of a SAGIN that can enhance existing networks’ resilience and provide critical connectivity to users requiring uninterrupted and quality network services. As illustrated in Fig. 1, UAVs can provide or enhance network

access for users in unserved and underserved areas or users in adverse and overload network conditions. As an aerial base station (BS), UAVs can be considered as a general high/low altitude platform stations (HAPS/LAPS) system [1] to enhance the coverage of satellite spot beams, which are subject to obstructions by rains, clouds, or other atmospheric conditions. UAVs can mitigate the connection interruptions or outages caused by malfunctioning terrestrial BSs [2]–[4]. UAVs can also be dispatched to offload high data traffics on a terrestrial network (TN) [5]–[8]. These representative scenarios well demonstrate the critical assisting roles of UAVs in a SAGIN.

However, the great promises of UAV-assisted SAGINs come with real-world challenges. First, for example, the modelling of the satellite networks, UAVs, and TNs needs to be made in accordance with key quality-of-experience (QoE) requirements, such as throughput, network outage, and fairness. Second, the use of network resources in all network segments needs to be jointly optimized. Third, the deployment of a UAV fleet needs to consider real-world factors, such as altitude keeping and trajectory planning, which can affect the problem modelling and performance. These requirements currently have not been extensively addressed in the literature in the context of UAV-assisted SAGINs. Recent survey papers as shown in Table II do not cover all topics for a SAGIN system model, such as UAVs, satellite components, ground components, as well as problem formulation and technical comparison. For example, authors in [9] discussed the overall use of reinforcement learning (RL) in communication networks, where the essential elements required in UAV-assisted SAGIN, such as satellite communication, ground components, problem formulation, and technical evaluation and comparison, are not addressed. In [10], the generic architectures using SAGINs in 5G network are discussed without providing a consistent formulation and evaluation of problems with the use of UAVs and ground components. In [11], the generic deployment overview of SAGINs is made, but no technical comparisons are made. Furthermore, only a portion of these papers discusses QoE metrics, although the metrics are application-specific. More importantly, the recent learning-based algorithmic approaches used in SAGINs have not been systematically discussed in these works.

Most of the state-of-the-art works in the literature on SAGIN are focused on the use of RL approaches, while the heuristic approach has hardly been addressed. Furthermore, some research efforts address UAV network challenges from the non-learning perspective, such as in [12]–[18] which are

Atefeh Hajijamali Arani and Yeying Zhu are with the Dept. of Statistics and Actuarial Science, University of Waterloo, ON N2L 3G1, Canada (e-mail: ahajijam@uwaterloo.ca; yeying.zhu@uwaterloo.ca).

Peng Hu is with Digital Technologies Research Centre, National Research Council Canada, Waterloo, ON N2L 3G1, Canada, and also with Dept. of Statistics and Actuarial Science, University of Waterloo, ON N2L 3G1, Canada. (Corresponding author email: Peng.Hu@nrc-cnrc.gc.ca)

developed based on successive convex approximation, penalty-based algorithms, and spatial average throughput for general and single UAV scenarios. In the same context, the authors in [19] model the problem of 2D placement of UAVs and channel allocation as a non-convex problem which is decoupled into two sub-problems. To solve the problem, the difference between convex functions optimization and quadratic transformation technique's are adopted. It is assumed that ground users are served by UAVs which are connected to the core network through a ground BS. These non-learning-based solutions may not be tractable for very complex and dynamic environments with high numbers of users and multiple UAVs. On the other side, they require some prior knowledge about the system (e.g. the locations of users) which is impractical for real-time solutions. In this regard, learning algorithms can assist in solving problems iteratively through learning from the system with low complexity and without the need for the full prior information of the system. Furthermore, the trajectories of UAVs are often modelled in a two-dimensional (2D) deployment scenario. However, in a real-world setup, three-dimensional (3D) deployment is required to be considered. The 2D and 3D deployments will change the trajectory planning of UAVs and have implications on affecting various performance metrics. The evaluation of the applicable algorithmic approaches under 2D and 3D scenarios needs to be made. On the other hand, some assumptions which are made at the level of users may be far from reality, such as statistic users and fixed user-BS association. Thus, it is required to consider the user's mobility assumptions.

This paper serves two purposes: an up-to-date review of the major methods in the UAV-assisted SAGIN is provided, and detailed comparison and analysis of these methods based on the RL, deep RL (DRL), satisfaction-based learning and heuristic approaches will be performed. The contributions are summarized in the following highlights.

- Our paper provides complete technical coverage of the UAV-assisted SAGIN as shown in Table I.
- We give an update-to-date discussion on applicable learning algorithms for UAV-assisted SAGIN.
- We provide a consistent and systematic evaluation of the algorithmic approaches with real-world deployment considerations in essential QoE metrics.
- We formulate the generic UAV-assisted SAGIN problem with implementations considering 2D and 3D UAV trajectory designs.

The remainder of the paper is structured as follows. In Section II, we review some recent developments of SAGINs. Section III overviews the RL approach and discusses the representative Q-learning and multi-armed bandit (MAB) algorithms for SAGINs. Section IV discusses the DRL approach for SAGINs. Section V discusses the satisfaction-based learning approach for SAGINs. In Section VI, the particle swarm optimization (PSO) based heuristic approach for SAGINs is discussed. The formulation of a joint optimization problem is presented in Section VII. Evaluation of these algorithmic approaches and open challenges are discussed in Section VIII. The conclusive remarks are made in Section IX.

II. OVERVIEW OF SAGINs

SAGIN is a recently proposed architecture [11] leveraging the space, aerial, and ground components. The space components may include geostationary (GEO), medium-Earth-orbit (MEO), and low-Earth-orbit (LEO) satellites. The aerial components may include HAPS/LAPS systems, such as stratospheric balloons, airships, and UAVs. The ground networks may include various telecommunications network while a cellular network is the typical option used. Fig. 1 shows typical scenarios where satellites, UAVs, and ground networks are integrated into a SAGIN, where the essential links between satellites, UAVs, and cellular base stations are shown. Due to the breadth of the SAGIN topic, here we capture the key characteristics of a SAGIN and formulate a generic optimization problem considering UAV deployments and key QoE metrics, which can be extended to SAGIN variations.

SAGIN is a promising architecture that can address the recent developments in satellites and terrestrial networks and lead to 6G [20], but it also introduces many challenges from individual segments to an integrated system. For the aerial network perspective, a SAGIN can be assisted with UAVs being aerial BS nodes. Baltaci *et al.* [21] discussed the connectivity technologies and challenges based on satellite communication, HAPS networks, and air-to-air (A2A) links. Although UAVs being aerial BSes can provide a better line-of-sight (LoS) coverage to ground users, their path planning needs to be made. The placement of UAV-based BS has been explored in [22]. A DRL is proposed in [23] to address the UAV path planning for mobile edge computing scenarios. The computation system poses another challenge where the computation resources from space, aerial, and ground components need to be made coherently. A scheduling scheme for computation offloading in SAGINs is proposed in [24]. A cooperative scheme for utilizing the computation resources for different scenarios is proposed in [20]. A deep Q-learning algorithm for traffic offloading is explored in [25]. Heuristic methods represent another learning-based approach for solving UAV-related problems. For example, a PSO path planning scheme is explored in [26]. The adaptive PSO task scheduling scheme for a SAGIN is discussed in [27]. The UAV placement and coverage maximization problems using PSO are studied in [28], [29]. We can see that the both learning algorithms have recently been adopted in UAV and SAGIN settings. However, due to different setups and problem domains in the existing works, we can hardly see and compare actual performance in typical deployment scenarios shown in Fig. 1 between these algorithms. As learning algorithms are promising to solve SAGIN-related problems, an overview from an algorithmic perspective is lacking in the current literature. When used as a toolbox for the SAGIN research, it is essential to provide a systematic overview of these algorithms and discuss how they can be applied to the generic SAGIN system model.

III. REINFORCEMENT LEARNING FOR SAGINs

RL is considered as a feedback-based ML technique that agents learn to interact with the environment through selecting actions and observing their outcomes [30], [31]. Theoretically,

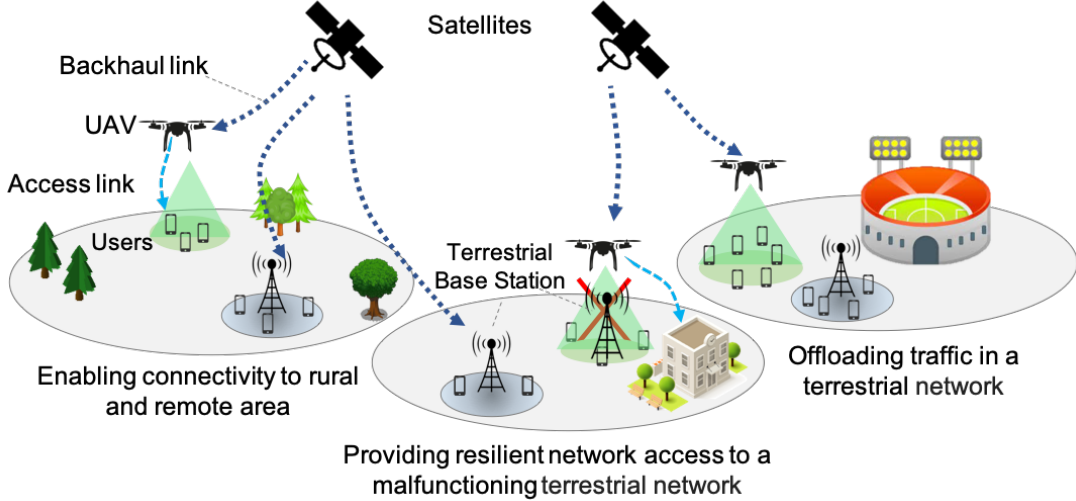


Fig. 1: Example use cases of employing a UAV-assisted SAGIN for enabling network access to terrestrial network users, who are located in rural/remote areas and malfunctioning/overloaded terrestrial networks. UAVs in these cases are considered as aerial base stations.

TABLE I: Overview of Existing Survey Papers

Topic	References	Robots/UAVs	Satellite Components	Ground Components	Problem Formulation	Technical Comparisons
Survey on DRL in Communications Networks	[9]	Yes	No	No	No	No
Architectural overview on SAGIN in 5G networks	[10]	No	Yes	No	No	No
Developments overview on SAGIN from network design, resource allocation, to performance evaluation	[11]	Yes	Yes	No	No	No
Our paper		Yes	Yes	Yes	Yes	Yes

RL algorithms use the Markov decision process (MDP) framework composed of an environment and a set of agents [32]. Agents face a trade-off between *exploration* and *exploitation*, in which each agent exploits the action with the highest reward and explores its other actions to enhance the estimations of actions' rewards. The main elements of RL algorithms can be defined as follows:

- *Agent*: A decision maker that can explore the environment to take an action, and receives a reward associated to its action.
- *Environment*: A situation that an agent operates and is surrounded by.
- *Action*: An action is a decision taken by an agent.
- *Reward*: A feedback that an agent receives from the environment after taking an action to evaluate its performance.
- *State*: It is the current situation of an agent returned by the environment in effect of its selected action.
- *Value Function*: It indicates the expected return with a discount factor for each state, given a certain policy.

Among different RL algorithms, we focus on MAB and Q-learning algorithms which are mostly used in literature to solve problems in various applications.

A. Q-learning Algorithm

Q-learning algorithm is known as one of the most popular algorithm among RL algorithms [30], [33]. In this regard, we intend to provide a review on the applications of Q-learning algorithms in UAV enabled systems. For a better understanding of its application, we first present the fundamentals of Q-learning algorithm.

Let π denote a *policy* for an agent which maps a state to an action. The goal is to find an optimal policy which maximizes

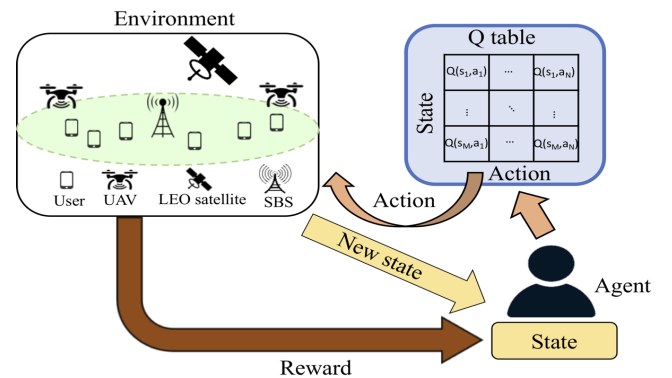


Fig. 2: Learning structure based on the Q-learning algorithm.

the expected sum of discounted reward instead of maximizing the immediate reward. Here, we define the value function $\mathcal{V}_\pi(s, a)$ for policy π and taking action a in state s which can be given as follows [9]:

$$\mathcal{V}_\pi(s, a) = \mathbb{E}_\pi \left[\sum_{t=0}^{\infty} \gamma_{\text{QL}} r(t) | s_0 = s \right] = \mathbb{E}_\pi [r(t) + \gamma_{\text{QL}} \mathcal{V}_\pi(s(t+1), a(t+1)) | s_0 = s], \quad (1)$$

where γ_{QL} and $r(t)$ are a discount factor and the reward at time t , respectively. We can observe that the value function can be decomposed into two parts including the immediate reward and the discounted value of successor state. Accordingly, we aim at obtaining the optimal policy that maximizes the value function as

$$\mathcal{V}_\pi^*(s, a) = \max_{a_t} \left\{ \mathbb{E}_\pi [r(t) + \gamma_{\text{QL}} \mathcal{V}_\pi(s(t+1), a(t+1))] \right\}. \quad (2)$$

Let $Q_\pi^*(s, a) \triangleq r(t) + \gamma_{\text{QL}} \mathbb{E}_\pi [\mathcal{V}_\pi(s(t+1), a(t+1))]$ be the optimal Q-function. Thus, the optimal value function can be represented by $\mathcal{V}^*(s, a) = \max_\pi Q_\pi^*(s, a)$. To find the optimal values of Q-function $Q_\pi^*(s, a)$, an iterative process can be used. Therefore, the Q-function can be updated as follows:

$$Q(s(t), a(t)) \leftarrow Q(s(t), a(t)) + \alpha_{\text{QL}}(t) [r(t) + \gamma_{\text{QL}} \max_{a'} Q(s(t+1), a') - Q(s(t), a(t))]. \quad (3)$$

The update rule in (3) finds the Temporal Difference (TD) between the predicted Q-value $r(t) + \gamma_{\text{QL}} \max_{a'} Q(s(t+1), a') - Q(s(t), a(t))$ and the current value $Q(s(t), a(t))$. Here, $Q(s(t), a(t))$ is the Q-function (or the learned action-value function) for taking action $a(t)$ in state $s(t)$ at time t . Parameter $\alpha_{\text{QL}}(t)$ denotes the learning rate which shows the impact of new information to the existing value, and it is chosen according to the following conditions: $\alpha_{\text{QL}}(t) \in [0, 1]$, $\lim_{t \rightarrow \infty} \sum_{t=0}^{\infty} \alpha_{\text{QL}}(t) = +\infty$, and $\lim_{t \rightarrow \infty} \sum_{t=0}^{\infty} (\alpha_{\text{QL}}(t))^2 < \infty$.

As illustrated in Fig. 2, Q-learning algorithm is based on a Q-table for each agent at each step. The table consists of the combinations of states and actions, in which the dimension of the table is $|\text{Actions}| \times |\text{States}|$, where $|\mathcal{A}|$ denotes the cardinality of set \mathcal{A} . An example for the state and action of an agent in path planning problem can be the location of the agent in a given area and its movement in different directions, respectively [4], [34]. Algorithm 1 shows the pseudocode for the Q-learning algorithm in a multi-agent system with the $|\mathcal{B}|$ agents where \mathcal{B} is the set of agents. The subscript b represents the elements of RL algorithm for agent b , e.g., $a_b(t)$ denotes the action of agent b and $s_b(t)$ is the state of agent b at time t . Each agent b interacts with the environment, and selects action $a_b(t) \in \mathcal{A}_b$ at time $t \in \{1, \dots, N\}$ with duration T_s , where \mathcal{A}_b is the set of actions for agent b , and N is the total number of time instants. Let \mathcal{S} denote the set of all possible states. Then, it transits from state $s_b(t)$ to a new state $s_b(t+1)$, and receives the reward $r_b(t)$. Furthermore,

Algorithm 1 : Q-learning Algorithm

```

1: Initialization:  $Q(s_b(t), a_b(t)) = 0$  for all  $s_b(t) \in \mathcal{S}$  and  $b \in \mathcal{B}$  for  $t = 0$ ,
2: while  $t < N$  do
3:    $t \leftarrow t + 1$ 
4:   for  $\forall b \in \mathcal{B}$  do
5:     if  $\text{rand}(\cdot) < \epsilon$  then
6:       Select action  $a_b(t)$  randomly
7:     else
8:       Select action  $a_b(t) = \text{argmax}_{a'_b} Q(s_b(t), a'_b)$ 
9:     end if
10:    Calculate reward  $r_b(t)$ , and observe the state  $s_b(t+1)$ 
11:    Update Q-function according to (3)
12:   end for
13: end while

```

an iterative Q-function is updated under stochastic state and the action taken by the agent using a learning rate α_{QL} and a discount factor γ_{QL} as described in (3). The learning rate $\alpha_{\text{QL}}(t) \in [0, 1]$ indicates that the impact of the old value of the action-value function on the current update. Parameter γ_{QL} determines the impact of the future reward on the system and balances the importance of short-term and long-term reward which is in the range $[0, 1]$. Note that, by allowing $\gamma_{\text{QL}} \rightarrow 0$ it leads to considering the immediate reward of an action. On the contrary, by allowing $\gamma_{\text{QL}} \rightarrow 1$, the future reward has the same weight as the immediate reward. After updating the Q-function, then the agent selects the action with the highest Q-value based on a certain probability.

Learning algorithms can play an essential role in improving the performance of integrated networks. Several work investigate using Q-learning algorithms to design UAV trajectory and path planning in order to meet the QoE requirements and system performance targets such as: maximum coverage and throughput, minimum interference and best QoE.

In [34], a trajectory optimization problem is studied through a RL algorithm which consists of using a Q-learning based approach for a scenario where multiple UAVs aim at maximizing the sum rate of ground users. The UAVs are trained to determine their trajectories according to the system topology, and try to decrease their distances to the users. This can be resulted in enhancing the communication link quality. The reward function of each UAV captures three terms, including the sum rate of users associated to the UAV, the distance between the UAV and its final location, and an activation function to assure the safety of the UAVs. It is also assumed that the altitudes of UAVs are fixed to a certain value. Finding the optimal trajectory of a single UAV flying at a constant altitude is studied in [35]. Using a Q-learning based algorithm, the UAV learns its 2D location to maximize the sum rate of ground users in the environment which contains a cuboid obstacle with a height equal to the altitude of the UAV. The reward function includes the sum rate and a negative component which avoids the UAV stepping outside the area. Moreover, an additional term is added in the reward function for the UAV safety check, in which it can return to its initial

location within the flying time limit.

To maximize the sum rate while satisfying the rate requirement of users, a three-phase mechanism is developed in [36]. In the first phase, a Q-learning algorithm is applied to determine the locations of UAVs according to the initial locations of users. Then, using a real dataset, the trajectories of users are determined, and then their future positions are predicted. Finally, a Q-learning scheme is proposed to find the transmit power and predict the locations of UAVs based on the mobility of users in the network. The reward function of the Q-learning corresponds to the instantaneous sum rate of the users. The authors in [37] investigate the placement of multiple UAVs to maximize the sum mean opinion score which evaluates the satisfaction of users. To solve the problem, a three-step approach is provided. First, a genetic algorithm based on K-means is applied to find the cell partition of users, in which the users are partitioned into different clusters, and a UAV is deployed for each cluster. Next, by using a Q-learning algorithm, the locations of UAVs are initially determined when users are static. Then, for the case that users are roaming, a Q-learning based movement algorithm is developed. A discrete reward function is used based on the instantaneous mean opinion score of the users. Authors in [38] investigate the problem of resource management in a multi-UAV network to efficiently allocate power and channel. The objective is to maximize a reward function, which captures power and throughput, to improve the energy efficiency of the system through allocating power and channel. Furthermore, they consider predefined flight plans for UAVs. In the cellular network context, the authors in [39] address the trajectory design problem for a single UAV to maximize the satisfied users. The satisfactions of users are determined based on the completion of user's request within an endurance time. Compared to other works, they consider two types of users including ground and aerial users. To solve the problem, a double Q-learning algorithm is used which yields an improvement over a Q-learning based algorithm.

B. MAB Algorithm

In a MAB approach, each agent (or bandit) has multiple arms (or actions). After choosing an action from its set of actions, it observes a reward associated to the selected action.

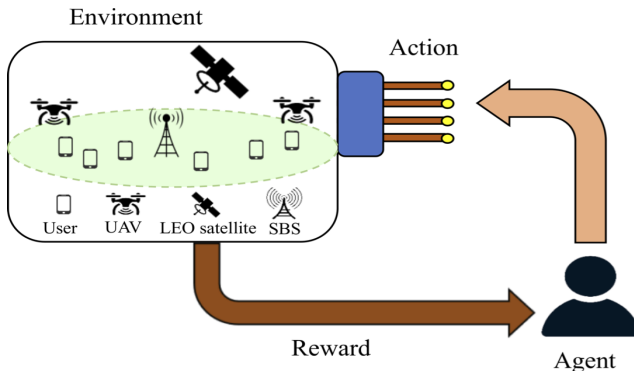


Fig. 3: Learning structure based on MAB algorithm.

Algorithm 2 : MAB Algorithm

```

1: Initialization:  $\bar{R}_{b,i}(t) = 0, n_{b,i}(t) = 0$  for  $t = 0, \forall b \in \mathcal{B},$ 
    $\forall a_{b,i} \in \mathcal{A}_b$  and  $i \in \{1, \dots, |\mathcal{A}_b|\}$ 
2: while  $t < N$  do
3:    $t \leftarrow t + 1$ 
4:   for  $\forall b \in \mathcal{B}$  do
5:     if  $\exists a_{b,i} \in \mathcal{A}_b$  s.t.  $n_{b,i}(t) = 0$  then
6:       Select arm  $a_b^{\text{MAB}}(t) = a_{b,i}$ 
7:     else
8:       Select arm  $a_b^{\text{MAB}}(t)$  according to (4)
9:     end if
10:    Calculate  $R_b(t)$ 
11:    for  $\forall a_{b,i} \in \mathcal{A}_b$  do
12:      Update  $a_{b,i}(t)$  as:  $n_{b,i}(t) = n_{b,i}(t - 1) +$ 
         $\mathbb{1}_{\{a_{b,i} = a_b^{\text{MAB}}(t)\}}$ 
13:      Update  $\bar{R}_{b,i}(t)$  as:
        
$$\bar{R}_{b,i}(t) = \frac{n_{b,i}(t-1)\bar{R}_{b,i}(t-1) + \mathbb{1}_{\{a_{b,i} = a_b^{\text{MAB}}(t)\}} R_b(t)}{n_{b,i}(t)}$$

14:    end for
15:  end for
16: end while

```

Then, the agent updates the average reward of the selected action [40]. However, this approach does not require any prior knowledge on the actions' rewards. Therefore, agents try to explore different actions. Fig. 3 illustrates the structure of MAB algorithm. One approach to solve MAB based problems is upper confidence bound (UCB) policy in which the action is chosen as [41]:

$$a_b^{\text{MAB}}(t) = \operatorname{argmax}_{a_{b,i} \in \mathcal{A}_b} \left\{ \bar{R}_{b,i}(t) + \sqrt{\frac{2 \ln t}{n_{b,i}(t)}} \right\}, \quad (4)$$

where \mathcal{A}_b and $\bar{R}_{b,i}(t)$ represent the action set of agent b and the average reward from action $a_{b,i} \in \mathcal{A}_b$ for player b at time t , respectively. Parameter $n_{b,i}(t)$ is the number of times that action $a_{b,i}$ has been selected by agent b until time t . The pseudocode for the MAB algorithm is presented in Algorithm 2.

The main difference between the MAB and Q-learning algorithm is that the MAB algorithm does not recognize the state of the system, and it is only based on actions. On the contrast, the Q-learning algorithm depends on the state of the system to update the Q-value function, and it is an action-space states based algorithm.

Authors in [42] address the joint backhaul and access link optimization for a SAGIN. The problem of satellite-BS association in backhaul links are solved to maximize the throughput. In access links, the problem of BS-user association, 3D trajectory of UAVs, and resource management for small cell BSs (SBSs) and UAVs are investigated which aims at improving the system throughput. To solve the access link problem, a UCB based mechanism is utilized. On the other hand, the load of SBSs and UAVs are considered as the function of user's required rate to capture user heterogeneity. In the same context, the authors in [4] leveraged the MAB mechanism to take into account provisioning fairness among users and bal-

ancing load among SBSs and UAVs. The proposed approach is compared to a Q-learning based mechanism and yields better performance in terms of fairness, load and throughput. A UAV-assisted emergency communication solution is developed in [43]. The UAV acts as an aerial BS to provide communication service for ground users in a post-disaster area. The target is to find the optimal path to serve the maximum number of users. In this regard, the UAV task is formulated as an extended MAB, and two solutions based on the distance-aware UCB and ϵ -exploration algorithms are proposed.

In the context of anti-jamming strategy, the authors in [44] propose a MAB-based anti-jamming channel selection model for software defined UAV swarm systems. In [45], a set of UAVs serve ground users as edge computing servers. The objective is to minimize the delay of the offloaded tasks over time. To do that, the task offloading problem is modeled as a combinatorial MAB problem, and a combinatorial bandit UCB algorithm is developed. In [46], a UAV task offloading problem based on MAB is addressed. Then, a variance-reduced learning-aided task offloading scheme is developed. In the context of non-orthogonal multiple access (NOMA)-UAV systems, a MAB-based approach is used in [47]. A single UAV collects data from internet of things (IoT) sensors in the uplink direction. The objective of the problem is to maximize the sum rate of all sensors.

IV. DEEP REINFORCEMENT LEARNING FOR SAGINS

Although RL algorithms can be used to solve different types of complex decision-making problems in various fields, it yields degraded performance when state spaces and action sets are large. Hence, the problems with large and/or continuous states can be difficult to solve with traditional RL methods. DRL algorithms have been shown as a promising solution for tackling the RL limitations [51]. DRL can be treated as a combination of RL and function approximation. In this context, function approximation is used to approximate the Q-value function.

Among various deep learning algorithms, we review the most commonly used DRL which is deep Q network (DQN) proposed by Mnih et al. [52]. DQN uses deep neural networks (DNNs) to approximate Q-values. It is composed of two neural networks including evaluation net and target net [53]. The current state is considered as the input of the evaluation net, and its outputs are relevant to evaluated Q-values for all actions. The target net provides the target values for the evaluation net with the same structure as the evaluation net. However, there is a delay in updating the weights of the target net to enhance the stability and decrease the correlation between the Q-values of evaluation and target nets. The DNNs are trained by means of optimizing the loss function

$$l(w) = E[(y(t) - Q(s(t), a(t); w_{\text{eval}}))^2], \quad (5)$$

where $Q(s, a; w_{\text{eval}})$ is the evaluated Q-value from the evaluation Q net with the weights of w_{eval} . Here, $y(t)$ is the target Q value from the target Q net which can be obtained by

$$y(t) = r(t) + \gamma \max_{a'} Q(s(t+1), a'; w_{\text{target}}), \quad (6)$$

Algorithm 3 : DQN Algorithm

```

1: Initialization: replay memory  $M_b$  to capacity  $M_c$ ,  $w_b^{\text{target}}, w_b^{\text{eval}}$ , let  $w_b^{\text{target}} = w_b^{\text{eval}}, t = 0, \forall b \in \mathcal{B}$ 
2: for episode = 1 :  $N_{ep}$  do
3:   Initialize  $s_t$  for all agents
4:   while  $t < N$  do
5:     for  $\forall b \in \mathcal{B}$  do
6:       if  $\text{rand}(\cdot) < \epsilon$  then
7:         Select action  $a_b(t)$  randomly
8:       else
9:         Select action  $a_b(t) = \text{argmax}_{a_b} Q(s_b(t), a_b; w_{\text{eval}})$ 
10:      end if
11:      Observe reward  $r_b(t)$  and transit to state  $s_b(t+1)$ 
12:      Store the experience  $(s_b(t), a_b(t), r_b(t), s_b(t+1))$  in  $M_b$ 
13:      Sample random minibatch of transitions  $(s_b(j), a_b(j), r_b(j), s_b(j+1))$ 
14:      Set  $y_b(j) = r_b(j) + \gamma \max_{a'_b} (Q(s_b(j+1), a'_b; w_b^{\text{target}}))$ 
15:      Perform a gradient descent step on  $l_b(w_b^{\text{eval}}) = E[(y_b(j) - Q(s_b(j), a_b(j); w_b^{\text{eval}}))^2]$  with respect to the DQN parameter  $w_b^{\text{eval}}$ 
16:      Every  $N_c$  iterations set  $w_b^{\text{target}} = w_b^{\text{eval}}$ 
17:    end for
18:  end while
19: end for

```

where w_{target} is the parameter of the DNN, i.e., weights and biases. Parameter γ denotes a discount factor. To train the network, a replay memory is employed, in which each agent stores its experience (s_t, a_t, r_t, s_{t+1}) in the replay memory [54]. It allows the agent to learn from its earlier memories which contains its current state, action, reward, and next state. To select an action, an ϵ -greedy strategy can be used. Thus, a random action is chosen with a probability ϵ , and the optimal estimate action is selected with probability $1 - \epsilon$, as follows:

$$a(t) = \text{argmax}_a Q(s(t), a; w_{\text{eval}}). \quad (7)$$

Algorithm 3 presents the process of DQN approach in a multi-agent system, where the subscript b represents agent b . This algorithm can be deployed in a distributed manner, in which each agent can have its own DQN, and updates it based on the collected data. Parameter N_c denotes the delay for updating the weights of the target net. Fig. 4 shows the structure of the DQN algorithm.

DQN has been widely adopted in aerial networks to solve different problems such as trajectory design and resource management. In [55], the authors optimize the trajectory of a single UAV and scheduling of status update packets. They develop a DQN to minimize the weighted sum of age-of-information. In order to train the UAV, one fully connected layer with no convolutional neural networks is used. In [56], a double Q-learning based traffic offloading for SAGINs is proposed. In [57], a UAV-aided emergency communications is assumed to overcome the malfunctioning of a ground BS.

TABLE II: Recent works on algorithmic approaches for UAVs

Reference	Year	Addressed issues	Access/backhaul links	Resource management	Trajectory design	Q-learning	MAB	Space	Aerial (single/multiple UAVs)	Ground	User mobility
[42]	2021	Throughput	Access, backhaul	Power, channel	3D	✓	✓	✓	Multiple	✓	✓
[4]	2021	Load, throughput, fairness	Access, backhaul	Channel	3D	✓	✓	✓	Multiple	✓	✓
[19]	2019	Throughput	Access, backhaul	Channel	2D	-	-	-	Multiple	✓	-
[48]	2019	Throughput	Access, backhaul	-	2D	-	-	-	Multiple	✓	✓
[49]	2020	Throughput	Access, backhaul	Channel	-	Non-learning	Non-learning	✓	Multiple	✓	-
[38]	2020	Energy efficiency	Access	Power, channel	-	✓	-	-	Multiple	✓	-
[50]	2020	Throughput	Access, backhaul	Power	2D	Non-learning	Non-learning	-	Multiple	✓	-
[43]	2019	Battery consumption, throughput	Access	-	2D	-	✓	-	Single	-	-
[5]	2020	Throughput	Access	-	3D	✓	✓	-	Multiple	✓	-

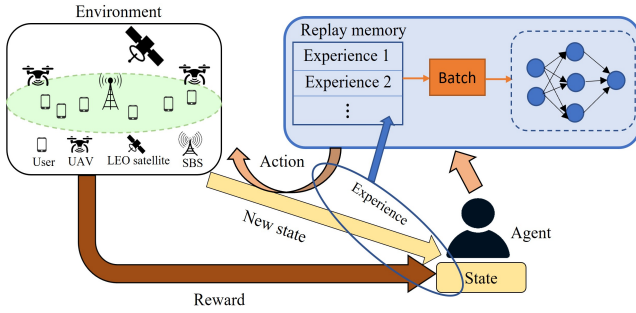


Fig. 4: Learning structure based on deep Q-learning algorithm.

In this regard, to maximize the number of the UEs served by the UAV, a DQN based algorithm is utilized to optimize the UAV's trajectory. In [58], a UAV is used as a mobile edge server to serve users. To optimize the trajectory of the UAV, a QoS-based approach is developed to maximize a reward function which captures the amount of offloaded tasks from users. To solve the problem, a DQN algorithm is developed. To dynamically allocate resources in heterogeneous networks (HetNets) and UAV networks, a DQN-based mechanism is developed in [59]. The system is composed of a macro BS and SBSs and a single UAV with considering a high mobility scenario for users. To model the DQN, 4 hidden layers with different neural units are used. In [60], a joint problem to find the UAVs' locations and manage the resources in a cooperative UAV network is investigated. To solve the problem, a DRL based mechanism combined with a difference of convex algorithm is adopted. For UAV-enabled wireless powered communication networks, a joint UAV trajectory planning and resource allocation mechanism is proposed in [61]. Accordingly, a DQL based strategy is developed to maximize the minimum throughput.

V. SATISFACTION BASED LEARNING FOR SAGINS

The satisfaction concept is proposed in [62], and its applications in the field of wireless communication are introduced in [63], [64]. The main difference between RL algorithms

and satisfaction based learning is that the RL algorithms aim at maximizing a reward function while satisfaction based learning schemes aim at satisfying the system [65]. Therefore, the satisfaction algorithms guarantee to obtain each agent a minimum reward value while improving the total reward of the system. Similar to the RL algorithms, we need to consider a set of agents and a reward function. Each agent b selects its action according to a probability distribution $\pi_b(t) = (\pi_{b,1}(t), \dots, \pi_{b,|\mathcal{A}_b|}(t))$, where \mathcal{A}_b is the set of actions for agent b . Here, $\pi_{b,i}(t)$ denotes the probability which agent b selects action $a_{b,i} \in \mathcal{A}_b$ at time t . In the satisfaction based approach, the satisfaction means that the observed reward for an agent is no less than a certain threshold. Let κ_b denote a satisfaction threshold for agent b . In this regard, each learning iteration of the satisfaction approach contains the following process:

- In the first iteration, each agent b selects its action randomly according to a uniform distribution, i.e. $\pi_{b,i}(t) = \frac{1}{|\mathcal{A}_b|}$, $\forall b \in \mathcal{B}$, $\forall a_{b,i} \in \mathcal{A}_b$ and $i \in \{1, \dots, |\mathcal{A}_b|\}$.
- For $t > 1$, if agent b is not satisfied with its received reward value, it may change its action based on the probability distribution $\pi_b(t)$; otherwise, it will keep its current action. Therefore, we define a satisfaction indicator $\varphi_b(t)$ for agent b at time t . Let $\Gamma_b(t)$ be the observed reward for agent b at time t , each player b computes $\varphi_b(t)$ as follows:

$$\varphi_b(t) = \begin{cases} 1, & \text{if } \Gamma_b(t) \geq \kappa_b(t) \\ 0, & \text{otherwise.} \end{cases} \quad (8)$$

- The agent obtains a reward according to its selected action.
- The probability $\pi_{b,i}(t)$ assigned to action $a_{b,i}$ is updated as follows:

$$\pi_{b,i}(t+1) = \begin{cases} \pi_{b,i}(t), & \text{if } \varphi_b(t) = 1 \\ L_b(\pi_{b,i}(t)), & \text{otherwise,} \end{cases} \quad (9)$$

Algorithm 4 : Satisfaction Based Approach

```

1: Initialization:  $t = 0$ ,  $\pi_{b,i}(t) = \frac{1}{|\mathcal{A}_b|}$ ,  $\varphi_b(0) = 0$ ,  $\forall b \in \mathcal{B}$ ,
    $\forall a_{b,i} \in \mathcal{A}_b$  and  $i \in \{1, \dots, |\mathcal{A}_b|\}$ 
2: while  $t < N$  do
3:    $t \leftarrow t + 1$ 
4:   for  $\forall b \in \mathcal{B}$  do
5:     if  $\varphi_b(t-1) = 1$  then
6:        $a_b(t) = a_b(t-1)$ 
7:     else
8:       Select the action  $a_b(t)$  according to  $\pi_b(t)$ 
9:       if  $\text{mod}(t, \tau_{b'}) = 0$  then
10:         $\kappa_b \leftarrow \kappa_b(1 - \Delta_{\kappa_b})$ 
11:       end if
12:     end if
13:     Calculate reward  $\Gamma_b(t)$ ,  $\varphi_b(t)$ , and  $\pi_b(t)$ 
14:   end for
15: end while

```

where $L_b(\pi_{b,i}(t))$ is given by

$$L_b(\pi_{b,i}(t)) = \pi_{b,i}(t) + \mu_b(t) \lambda_b(t) \left(\mathbb{1}_{\{a_b(t)=a_{b,i}\}} - \pi_{b,i}(t) \right), \quad (10)$$

where $\mu_b(t) = \frac{1}{1000t+1}$ and $a_b(t)$ denote the learning rate and the action played by agent b at time t , respectively. The parameter $\lambda_b(t)$ is computed as $\lambda_b(t) = \frac{\Gamma_{\max} + \Gamma_b(t) - \kappa_b(t)}{2\Gamma_{\max}}$, where Γ_{\max} is the maximum reward that agent b can achieve. However, in the realm of wireless communications, agent b might not be satisfied at its satisfaction threshold. In this regard, the agent can update the threshold as $\kappa_b \leftarrow \kappa_b(1 - \Delta_{\kappa_b})$ after each time instant interval $\tau_{b'}$, where $0 < \Delta_{\kappa_b} < 1$ is a constant coefficient to decrease the level of the satisfaction threshold.

Algorithm 4 presents the pseudocode for the satisfaction mechanism.

In [64], a fundamental concept for satisfaction problem named as satisfaction equilibrium is presented, in which all agents are satisfied. Satisfaction based learning approaches are used in other research areas for resource management in wireless networks. In [66], [67], satisfaction based approaches are used for frequency allocation with QoS constraints. In [68], a satisfaction based algorithm is developed to allow a set of transmitters to choose their transmit power levels aiming at ensuring a minimum transmission rate. For sleep mode switching in HetNets, distributed satisfactory schemes are developed in [69], [70].

Beyond optimizing ground networks through developing satisfactory solutions, the work in [5] utilizes a satisfaction mechanism to address the problem of the 3D placement of UAVs integrated into TNs to alleviate network overload conditions. In addition to the UAV placement for ground integrated networks, the satisfaction schemes can be used in SAGINs. In this framework, a satisfaction learning based scheme is investigated in [42] for jointly resource management and 3D UAV trajectory design problem.

VI. PSO FOR SAGINs

PSO is a heuristic algorithm which is based on the concept of population and evolution inspired by social behavior and movement [71]. The mechanism of PSO algorithm is to find the best solution in complicated systems through cooperation and competition between particles in a swarm. The PSO starts with a random set of solutions composed of N_p particles. Each particle $n_p \in N_p$ contains a solution of the problem which includes L elements. The position of each particle is updated according to its velocity. Let $V_{n_p}(t)$ and $X_{n_p}(t)$ denote the velocity and position of particle n_p , respectively. The velocity of an element $l \in L$ in particle n_p can be updated as follows:

$$V_{n_p}^{(l)}(t+1) = \phi V_{n_p}^{(l)}(t) + c_p \phi_p (X_{n_p}^{(l, \text{best})} - X_{n_p}^{(l)}(t)) + \quad (11)$$

$$c_g \phi_g (X^{(l, \text{Gbest})} - X_{n_p}^{(l)}(t)), \quad (12)$$

where ϕ denotes the inertia weight which is employed to control the impact of the previous history of velocities on the current particle's movement. Parameters c_p and c_g are personal and global learning coefficients, respectively. Here, ϕ_p and ϕ_g denote two random positive numbers which are uniformly distributed in the interval $[0, 1]$. Therefore, the position of element l in particle n_p is updated as follows:

$$X_{n_p}^{(l)}(t+1) = X_{n_p}^{(l)}(t) + V_{n_p}^{(l)}(t+1). \quad (13)$$

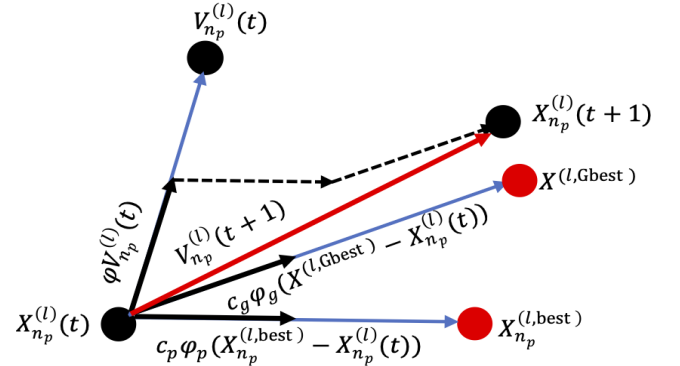


Fig. 5: Illustration for updating the position of an element in PSO algorithm.

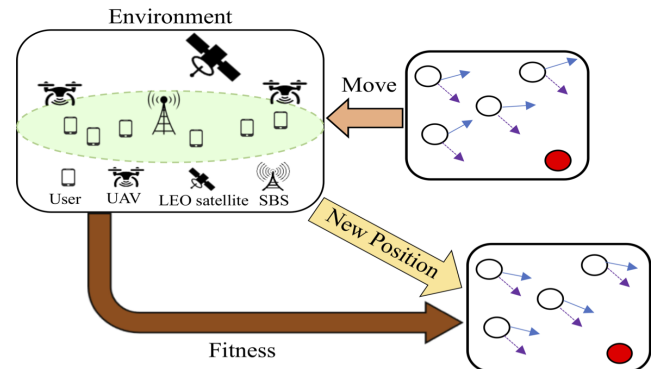


Fig. 6: Learning structure based on PSO algorithm.

Algorithm 5 : PSO Algorithm

```

1: Initialization:  $t = 0$ , initialize the position and velocity
   of all particles,  $X_{n_p}^{(l,\text{best})} =$ 
2: while  $t < N$  do
3:    $t \leftarrow t + 1$ 
4:   for  $\forall n_p \in N_p$  do
5:     Calculate the reward function
6:     if  $\Gamma_{n_p}(t) > \Gamma_{n_p}^{\text{best}}$  then
7:        $\mathbf{X}_{n_p}^{\text{best}} \leftarrow \mathbf{X}_{n_p}(t)$ 
8:        $\Gamma_{n_p}^{\text{best}} \leftarrow \Gamma_{n_p}(t)$ 
9:     end if
10:    if  $\Gamma_{n_p}(t) > \Gamma^{\text{Gbest}}$  then
11:       $\mathbf{X}^{\text{Gbest}} \leftarrow \mathbf{X}_{n_p}(t)$ 
12:       $\Gamma^{\text{Gbest}} \leftarrow \Gamma_{n_p}(t)$ 
13:    end if
14:  end for
15:  for  $\forall n_p \in N_p$  do
16:    for  $\forall l \in L$  do
17:      Update the velocity  $V_{n_p}^{(l)}(t)$  according to (11)
18:      Update the position  $X_{n_p}^{(l)}(t)$  according to (13)
19:    end for
20:  end for
21: end while

```

$X_{n_p}^{(l,\text{best})}$ and $X^{(l,\text{Gbest})}$ denote the best position of element l in particle n_p and among all particles, respectively. Furthermore, we define vector $\mathbf{X}_{n_p}(t) = (X_{n_p}^1(t), \dots, X_{n_p}^L(t))$, $\mathbf{X}_{n_p}^{\text{best}} = (X_{n_p}^{(1,\text{best})}, \dots, X_{n_p}^{(L,\text{best})})$, and $\mathbf{X}^{\text{Gbest}} = (X^{(1,\text{Gbest})}, \dots, X^{(L,\text{Gbest})})$. Let $\Gamma_{n_p}(t)$, $\Gamma_{n_p}^{\text{best}}$, Γ^{Gbest} denote the utility function for particle n_p at time t , the best utility of particle n_p , and the global best utility, respectively. Fig. 5 shows an illustration for updating the position of element l in particle n_p .

In the context of maximizing throughput and extending coverage for ground users, heuristic algorithms such as PSO can play a key role in solving UAV placement problems [72]. The major difference between PSO and RL algorithm is that PSO benefits from the population based behaviour and the best solution is shared among the particles in the system, while the latter tries to maximize the expected cumulative reward for each agent in the population. Here, we focus on research works that are based on PSO methods. A PSO based UAV placement is studied in [28], while the number of deployed UAVs are minimized so that the QoS requirements of users are satisfied. Initially, the number of UAVs to serve all users is estimated based on the capacity constraint. In the same context, a PSO based approach is utilized in [29] to maximize the coverage probability of UAVs through optimizing their 3D locations. The authors in [73] investigate the problem of joint user association and UAV placement through utilizing PSO algorithm in order to maximize the number of satisfied users in the system. In the first phase, each user is associated to the BS with the highest SINR. Then the required bandwidth is allocated to the user in order to fulfill the user's requested data rate until all of the bandwidth are assigned to users. To optimize the locations of UAVs, a PSO based scheme

is developed, in which the cost function captures the users' satisfactions according to the minimum required data rate of users. Based on the new locations of UAVs, the user association and bandwidth allocated to users are updated.

Another potential application of UAVs is using in mobile edge computing network, in which they can perform as flying edge computing servers to offloaded tasks from users. The work in [74] takes into account the problem of energy consumption and delay minimization. To solve the problem, they utilize heuristic algorithms such as PSO.

VII. PROBLEM FORMULATION

In this section, we discuss how to implement the above-mentioned algorithms in real-world scenarios. The target is to maximize a predefined reward function adapted to the type of the problem. In the context of providing connectivity to ground users, most existing literature focuses on maximizing throughput and coverage probability. For instance, the works in [19], [42], [48]–[50] aim at maximizing the systems' data rates. However, these studies do not takes into account the fairness among users which is an important factor for evaluating the performance of a system.

On the other side, during high-traffic times, ground BSs can be overloaded resulting in degrading user throughput and increasing inter-cell interference. An alternative and efficient complement to traditional TNs is UAV deployment, in which the system configuration can be adapted to the traffic demand and system load due to the flexibility of UAVs in placement. Moreover, the load balancing among UAV BSs needs to be optimized to achieve a further improvement in spectral efficiency.

Let Ψ_k and \mathcal{K}_b denote the requested rate of user k and the set of users associated to BS $b \in \mathcal{B}$, respectively, where $\mathcal{B} = \mathcal{U} \cup \mathcal{S}$. Here, \mathcal{U} and \mathcal{S} are the set of UAVs and SBSs, respectively. The load of a BS is defined as [75]

$$\rho_b = \sum_{k \in \mathcal{K}_b} \frac{\Psi_k}{C_{b,k}} \triangleq f_b(\boldsymbol{\rho}), \quad (14)$$

where $C_{b,k}$ is the achievable data rate to user k provided by BS b . Here, function $f_b(\cdot)$ represents the load of BS b as a function of the loads of all the BSs, where $\boldsymbol{\rho} = (\rho_1, \dots, \rho_{|\mathcal{B}|})$, and \mathcal{B} is the set of all the BSs. To find the loads of the BSs, we use the fixed point iteration algorithm due to the fact that the function $f_b(\boldsymbol{\rho})$ is a standard interference function. One of the most widely-used fairness metric is Jain's fairness index which can be defined as follows [76]:

$$\mathcal{F} = \frac{(\sum_{k \in \mathcal{K}} \bar{C}_k)^2}{|\mathcal{K}|(\sum_{k \in \mathcal{K}} \bar{C}_k^2)}. \quad (15)$$

where \bar{C}_k and \mathcal{K} are the total data rate for user k and the set of users, respectively.

Here, we aim at maximizing the fairness while balancing load among UAVs flying over the particular area \mathcal{R} . Therefore, we define a reward function that captures the fairness among users and the load of BSs as follows:

$$\Gamma_b(t) = \Phi_b \mathcal{F}(t) + \psi_b(1 - \rho_b(t)), \quad (16)$$

TABLE III: System-Level Simulation Parameters

System Parameters		
Parameter	Value	
Number of satellites in the orbital plane	22	
Altitude of satellites	550 km	
Height of SBSs	15 m	
Height of users	1.5 m	
Maximum altitude of UAVs	121.9 m	
Carrier frequency/channel bandwidth per BS in backhaul links	28 GHz, 100 MHz	
Number of frequency channels	4	
Channel bandwidth in access link	56 MHz	
Noise power spectral density	-174 dBm/Hz	
Number of SBSs	4	
Total number of iterations (N)	5740	
T_s	1 sec	
Fixed point iterations	500	
v_{\min}, v_{\max}	0, 1.3 m/sec	
UAV's speed	10 m/sec	
h_{\min}, h_{\max}	22.5 m, 121.9 m	
Ψ_k	1.8 Mbps	
Φ_b, ψ_b	0.5, 0.5	
Population size for PSO	20	
Inertia Weight	0.9	
Personal and global learning coefficients	0.1, 0.1	
$\Delta \kappa_b, \tau_{b'}$	0.2, 200	
Batch size	64	
Replay memory size	600	
BS Parameters		
Parameter	Terrestrial BS	UAV
Transmit power	24 dBm	24 dBm
Reference path loss	LoS: 61.4 NLoS: 72 [77]	LoS: 61.4 NLoS: 61.4 [78]
Path loss exponent	LoS: 2 NLoS: 2.92	LoS: 2 NLoS: 3
Shadowing standard deviation	LoS: 5.8 NLoS: 8.7	LoS: 5.8 NLoS: 8.7

where the coefficients Φ_b and ψ_b are the weight parameters that indicate the impact of the fairness and load on the reward function, respectively. Our overall objective is to maximize the total system reward function by optimizing the trajectories of the UAVs and channel allocation at the BSs as given by the following optimization problem

$$\max_{\mathbf{q}(t), \mathbf{A}(t)} \sum_{t \in N} \sum_{b \in \mathcal{B}} \Gamma_b(t) \quad (17a)$$

$$\text{s.t. } (x_u(t), y_u(t)) \in \mathcal{R}, \quad \forall u \in \mathcal{U}, \quad (17b)$$

$$h_u(t) \in [h_{\min}, h_{\max}], \quad \forall u \in \mathcal{U}, \quad (17c)$$

$$\rho_b(t) = f_b(\boldsymbol{\rho}), \quad \forall b \in \mathcal{B}, \quad (17d)$$

$$0 \leq \rho_b(t) \leq 1, \quad \forall b \in \mathcal{B}. \quad (17e)$$

For the optimization problem (17), we consider several constraints. The constraints in (17b) and (17c) define the feasible area for the locations of the UAVs in the 3D space. The constraints in (17d) and (17e) are related to the definition of load. Here, $\mathbf{a}_u(t) = (x_u(t), y_u(t), h_u(t))$ denotes the 3D coordinate of UAV u at time t . h_{\min} and h_{\max} are the minimum and maximum altitude of the UAVs. $\mathbf{q}(t)$ and $\mathbf{A}(t)$ are the vector of all the BSs' transmit channels and the locations of all the UAVs, respectively.

VIII. SIMULATION RESULTS

To compare the performance of the PSO based and learning based schemes, we consider an area with a size of 500m \times 500m. A set of users are uniformly distributed in the system and move based on a random walk mobility model, in which the users select their speeds from the ranges $[v_{\min}, v_{\max}]$ and their movement angles from the ranges $[0, 2\pi]$. Parameters v_{\min} and v_{\max} indicate the minimum and maximum speed of the users, respectively. Furthermore, 4 SBSs are uniformly distributed in the system while they keep a minimum distance of 40 and 10 meters from another SBS and a user, respectively. We average our results over 100 montecarlo simulations. To associate the users to the BSs, we consider a policy based on the highest signal strength. The maximum altitude of UAVs is determined based on the Federal Aviation Administration (FAA) Part 107 rules. For backhaul connectivity, we consider a set of LEO satellites, in which they are uniformly distributed in a circular orbit. Table III summarizes the main system parameters used in the simulations.

For the performance comparison, we consider the following schemes in our simulations:

- *3D satisfaction-CA*: Each BS selects its transmission channel and also each UAV optimizes its 3D trajectory based on the satisfaction approach.
- *2D satisfaction-CA*: The altitude of each UAV is set to the maximum altitude, and the UAVs utilize the satisfaction approach for optimizing their 2D trajectories. Furthermore, all the BSs in the system use the satisfaction approach for channel allocation problem.
- *2D satisfaction*: The altitude of each UAV is set to the maximum altitude, and the 2D flying directions of the UAVs are optimized based on the satisfaction approach. The channels of all the BSs are selected randomly.
- *3D MAB-CA*: The BSs and the UAVs select their transmission channels and optimize their 3D trajectories based on the MAB algorithm.
- *2D MAB*: The UAVs fly at their maximum altitude and select their 2D movement direction using the MAB algorithm. Furthermore, all the BSs choose their channels randomly.
- *3D PSO*: The PSO algorithm is used to find the 3D locations of the UAVs. Moreover, the BSs select their channels randomly.
- *2D PSO*: The altitudes of the UAVs are set to the maximum altitude, and they use the PSO algorithm to find their 2D positions. Furthermore, all the BSs select their channels randomly.
- *Q-learning*: The UAVs fly at the maximum altitude, and they use the Q-learning algorithm to optimize their 2D positions. Moreover, the channels of the BSs are randomly selected.
- *DQN-CA*: The UAVs select their 3D trajectories and transmit channels using the DQN algorithm. The DQN uses a fully connected layer with 200 hidden nodes.

In the following, we provide the performance of the learning and PSO based algorithms for different number of users and UAVs, and address how they affect the BS and user levels

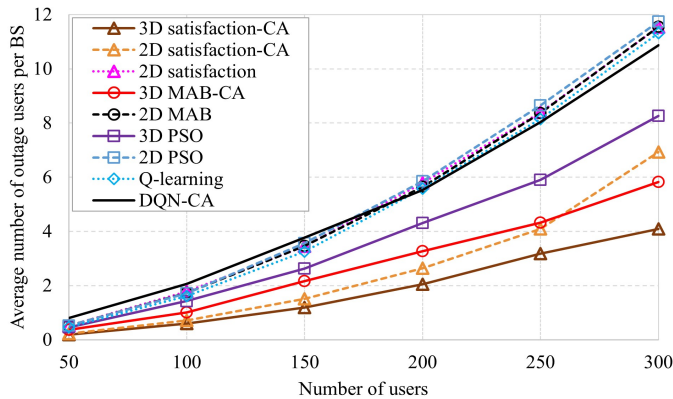


Fig. 7: Average number of outage users versus the number of users for a system with 4 SBSs and 4 UAVs.

performance, i.e., load, fairness, rate, and outage. Finally, we discuss their performances in the described system. Here, the solid curves belong to the 3D trajectories design algorithms, and the dashed curves refer to the 2D trajectories design mechanisms.

A. Performance Evaluation for Various Numbers of Users

For the first set of the results, we consider a system with 4 SBSs and 4 UAVs, and vary the number of users in the system from 50 to 300 users.

In Fig. 7, we compare the outage performance for the PSO and learning based approaches as a function of the number of users. Outage users defined as the set of users that receive the data rate less than the requested rate Ψ_k . This performance indicator is affected by the availability of resource at the BSs and the amount of resource to serve the requested rate from the BSs to the locations of the users. With knowledge of these factors, with increasing the number of users in the system, the remaining resource at the BSs decreases and more users experience the outage conditions. It can be observed that the 3D satisfaction-CA scheme can achieve better outage performance than the other algorithms. Furthermore, for the number of users lower than 250, the 2D satisfaction-CA has better performance compared to the 3D MAB-CA mechanism. However, for the high number of users, optimizing the altitudes of UAVs is more essential so that 3D MAB-CA performs better than the 2D satisfaction-CA. In addition, Fig. 7 also demonstrates that the performances of MAB, Q-learning, and PSO based algorithms for optimizing the 2D trajectories of UAVs are almost the same while for the high numbers of users, the DQN-CA algorithm yield lower outage users compared to the 2D based algorithms.

In Fig. 8, we consider the effect of the number of users in the system on the the average load per BS. One can observe that the 3D satisfaction-CA obtains better performance in terms of balancing load among the BSs. The main reason is that since the 3D satisfaction-CA provide a better performance in terms of spectral efficiency, it reduces average load in the system due to the inverse relation between load and rate according to (14). Moreover, with increasing the number of users, the

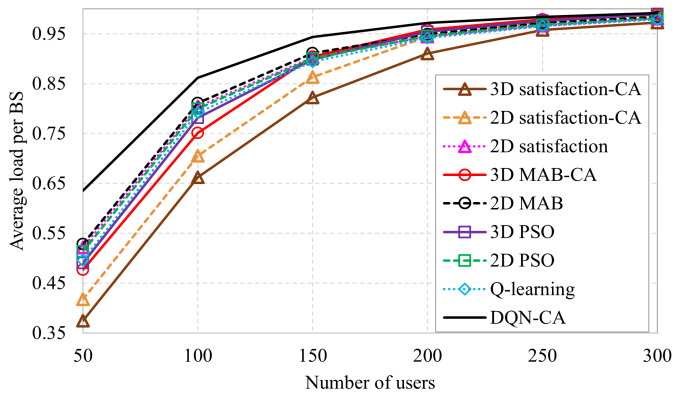


Fig. 8: Average load per BS versus the number of users for a system with 4 SBSs and 4 UAVs.

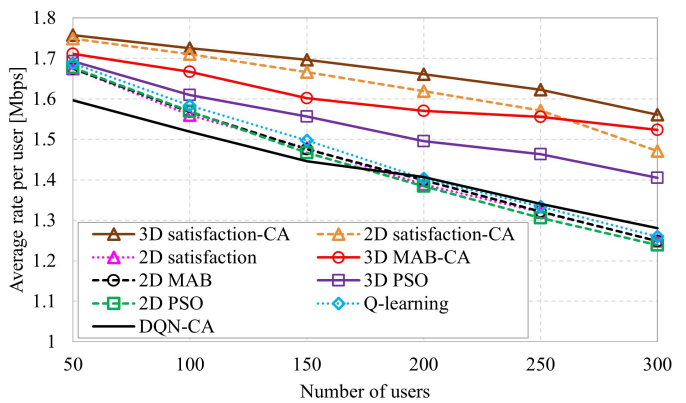


Fig. 9: Average rate per user versus the number of users for a system with 4 SBSs and 4 UAVs.

average load per BS increases which leads to increasing the number of outage users. However, for the high number of users, the performances of all the schemes are the same and approach to the maximum load, i.e. 1.

We continue by evaluating the effect of the number of users on the user's rate in Fig. 9. It is evident that the data rate is the function of load and the BSs and users locations. An insightful observation from Fig. 9 is that as the number of users increases, there is a notable decrease in the average rate per user due to overloading of the BSs (see Fig. 8). The instantaneous rate of a user is directly proportional to the SINR at the user; however, the overall served rate is related to the fraction of the resources at the BSs as well. Hence, the highly loaded BSs provide lower rate over time such that the long-term service rate experienced by the users are related to the load of the system. Furthermore, in the light load conditions, the users experience better SINR than the highly load conditions due to the lower interference. On the other hand, the average rate also depends on the resource management scheme at the BSs. Accordingly, the 3D satisfaction-CA approach significantly improves average rate per user compared to the other approaches due to the load balancing mechanism and efficiently resource management.

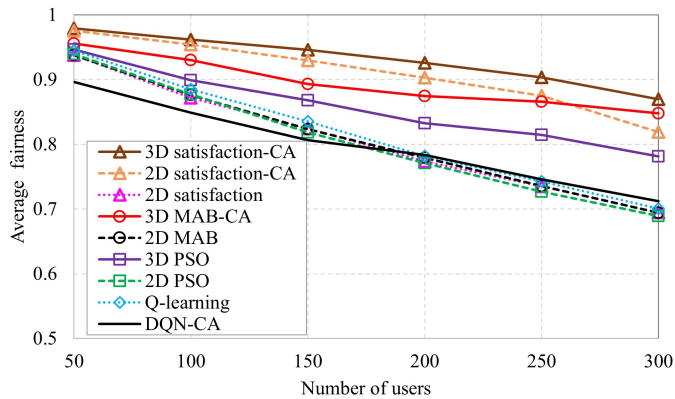


Fig. 10: Average fairness versus the number of users for a system with 4 SBSs and 4 UAVs.

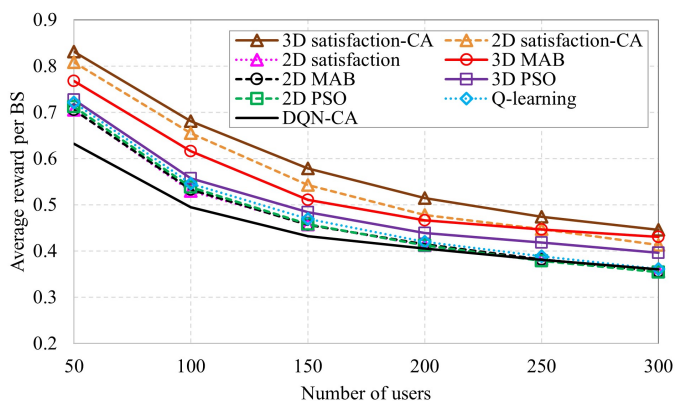


Fig. 11: Average reward versus the number of users for a system with 4 SBSs and 4 UAVs.

In Fig. 10, we compare the average fairness measure as given by the index that we have introduced in (15) for different number of users. It shows that the average fairness for all the schemes exhibit similar trends, in which it decreases with increasing the number of users. The key reason is that the amount of resource to assign to some users might be insufficient as the number of users increases. In addition, 3D satisfaction-CA can outperforms the other approaches in terms of fairness.

Fig. 11 shows the behavior of the reward function defined in (16). Since with increasing the number users, 3D satisfaction-CA outperforms the other schemes in terms of average fairness and load, it provides better average reward compared to the other approaches. We can observe that for the high number of users, the performances of the 2D MAB, PSO, Q-learning and DQN algorithms are almost the same.

B. Performance Evaluation for Various Numbers of UAVs

Here, we vary the number of UAVs in the system, and observe the performance of the learning and PSO mechanisms. Moreover, we set the number of users and the number of SBS to 150 and 4, respectively.

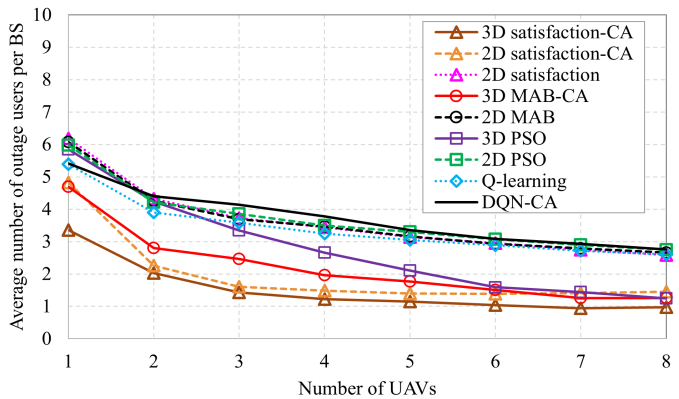


Fig. 12: Average number of outage users per BS versus the number of UAVs for a system with 4 SBSs and 150 users.

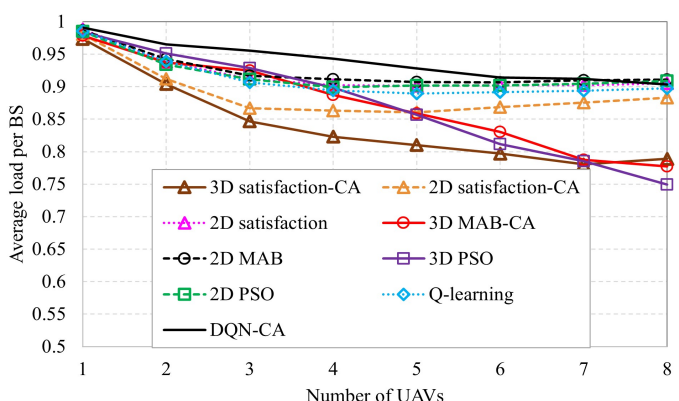


Fig. 13: Average load per BS versus the number of UAVs for a system with 4 SBSs and 150 users.

Fig. 12 illustrates the average number of outage users per BS versus the different number of UAVs. It shows that offloading the users from the highly loaded BSs to the lightly loaded BSs through increasing the number of UAVs helps to improve the average rate per user and decreasing the outage users. Fig. 12 also reveals that for the dense deployment of UAVs, the performances of the 3D based mechanisms and 2D satisfaction-CA scheme have almost the same performance and approach to 1 outage user per BS.

Fig. 13 demonstrates the impact of increasing the number of UAVs on the load balancing in the system. For the densely deployment of UAVs, the average load per BS decreases due to the offloading load from the highly loaded BSs to the lightly loaded BSs. Furthermore, we can see that for the number of UAVs less than 7 the 3D satisfaction-CA outperforms the others, while for the high number of UAVs the 3D PSO balances the load efficiently. On the other hand, increasing the number of UAVs may increase the interference in the system which results in increasing load as well. We can see this behaviour in 2D satisfaction-CA approach when the number of UAVs exceeds 6 so that the average load per BS increases.

In Fig. 14, we compare the performance of the PSO and learning based schemes in terms of average rate per user. We

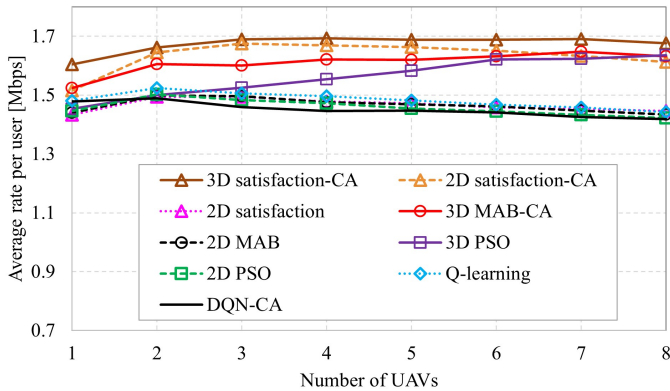


Fig. 14: Average rate per user versus the number of UAVs for a system with 4 SBSs and 150 users.

can observe that the 3D satisfaction-CA approach has better performance compared to the other approaches. Moreover, the 2D based algorithms except 2D satisfaction-CA and DQN-CA have almost the same performance. Furthermore, with increasing the number of UAVs in the system, the users have more opportunities to associate to lightly loaded BSs. Thus, their rates can be improved. However, as we mentioned it may increase the interference in the system.

The enhancement in the average fairness in Fig. 15 is consistent with the results in Fig. 14. The results in Fig. 15 show that as we increase the number of UAVs, the average fairness improves due to the increase of available resources. Thus, more UAVs means more covered users. However, the performance can be impacted by the increasing the co-channel interference in the system. Furthermore, it can be observed that the 3D satisfaction-CA algorithm achieves the highest fairness for all the number of UAVs, while the 2D MAB and 2D PSO, Q-learning, and DQN-CA have inferior fairness. This is because the 3D satisfaction-CA algorithm deal with the increasing interference through resource management at all the BSs and the trajectories designs of the UAVs so that the gap between it and 2D MAB and PSO, Q-learning, and DQN based algorithms increases. Furthermore, for the number of UAVs exceeds 7, the 3D MAB-CA and 3D PSO algorithms approach to the 2D satisfaction-CA and have slightly improvements on the fairness index over it.

Fig. 16 shows that the enhancement in average reward per BS through increasing the number of UAVs. It is worth noting that the performance of the 3D satisfaction-CA outperforms the other approaches due to efficiently optimizing the channel allocation and 3D trajectories of the UAVs. The DQN-CA and 2D based approaches including 2D satisfaction, 2D PSO, 2D MAB, and Q-learning have the lowest reward values compared to the other approaches. Furthermore, it can be seen that for the number of UAVs less than 6, the 2D satisfaction-CA outperforms the others except the 3D satisfaction based algorithm, while with increasing the number of UAVs, the 3D MAB-CA and 3D PSO yield higher reward values. This behaviour is due to that their performances are proportional to the load and fairness values which are illustrated in Fig. 13

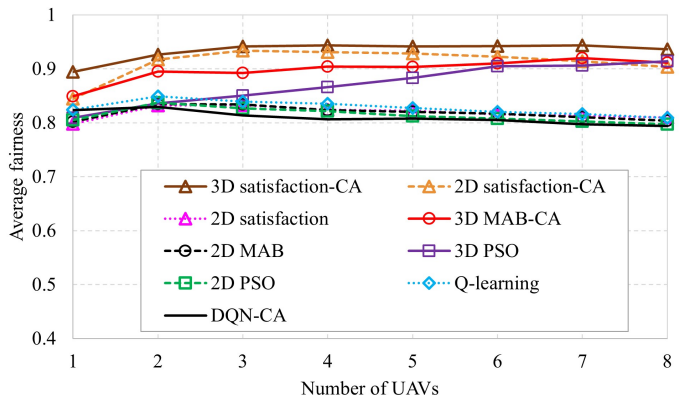


Fig. 15: Average fairness versus the number of UAVs for a system with 4 SBSs and 150 users.

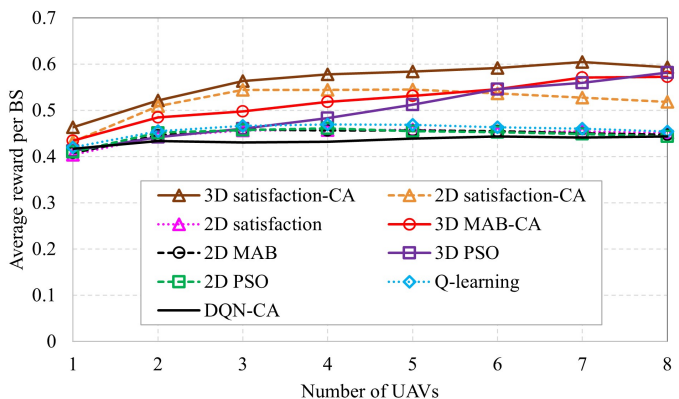


Fig. 16: Average reward versus the number of UAVs for a system with 4 SBSs and 150 users.

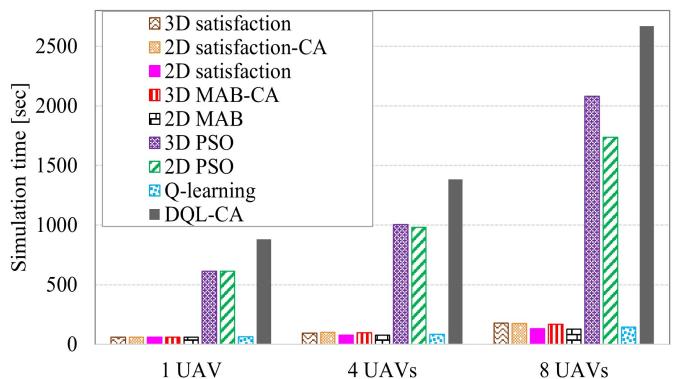


Fig. 17: Simulation time for 1, 4, and 8 UAVs and a system with 4 SBSs and 150 users.

and Fig. 15.

In Fig. 17 and Fig. 18, we evaluate the performance of the learning and PSO based algorithms in terms of time consumption for the simulations. We can observe that the DQN-CA and PSO based algorithms consume more time compared to the other algorithms due to having several neural networks and particles. Furthermore, the satisfaction and MAB

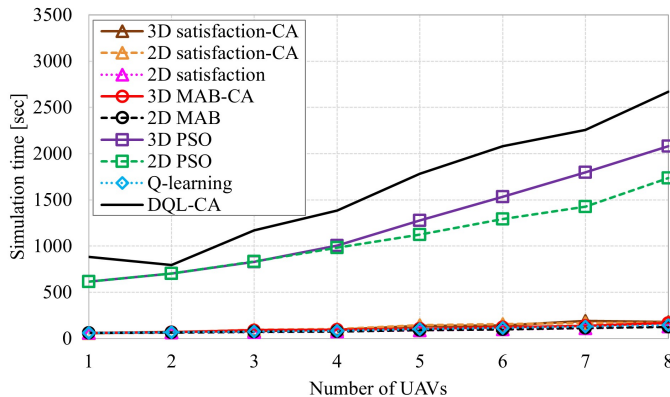


Fig. 18: Simulation time versus the number of UAVs for a system with 4 SBSs and 150 users.

based, Q-learning have the lowest simulation time.

C. Results Discussion

In this work, we consider the channel allocation problem combined with the trajectory design for the UAVs. According to the simulation results, we can observe that the 3D satisfaction-CA approach has a better performance compared to the other mechanisms. However, we need to select suitable values for the parameters of the satisfaction-based algorithm (e.g., satisfaction threshold). Since the 3D satisfaction-CA considers the channel allocation mechanism, it improves the performance of the system compared to the other 3D based approaches. In addition, the satisfaction based approaches avoid randomly changing actions when an agent is satisfied which results in better performance. Therefore, allocating resources in an efficient way is a crucial issue.

In addition, while we optimize the 2D locations of the UAVs, determining optimal altitudes for the UAVs is an important issue. In this regard, we can observe that the 3D based algorithms outperform the 2D based for the high numbers of UAVs. However, the performance of DQN-CA algorithm is lower than the other 3D based algorithm. The DQN structure used in this paper is similar to [55] for a system with only one BS which is a UAV. We use this structure for a more complex system which is our initial attempt to develop DQN into SAGINs. For our future work, we will continue to consider novel and more complex DQN algorithms and improve the computation overhead of the algorithm. Regarding the simulation time, the DQN-CA and PSO-based mechanisms consume more time compared to the other approaches due to having two neural nets and population-based property, respectively. Furthermore, with increasing the number of agents in the system, the simulation time for the learning-based and PSO algorithms increases. However, as a representative metaheuristic algorithm, the PSO-based approach can have a marginal performance difference compared to RL algorithmic approaches when the number of UAV is small. Due to its problem-independence feature, PSO can be easily transferred to other UAV-assisted SAGIN scenarios. The convergence time

taken in simulation can be further reduced with some schemes, such as random sampling of control parameters [79].

D. Open Challenges

Our work has provided a solid performance benchmark for recent algorithmic approaches for UAV-assisted SAGINs. However, there are still some open challenges for future contributions. The following are examples from the perspectives of system architectures, application scenarios, and algorithmic variations.

First of all, the detailed modelling using UAV networking where UAVs can collaborate with each other for message exchanges can be extended from our baseline system model. We realized that the networking functionality between UAVs can be optional and the assumption of system capability on UAV hardware and software is often required. For this reason, multi-hopping is not considered in our formulation. However, for a wide area coverage using many UAVs, multi-hopping and networking may be advantageous for UAV fleet operations, and the networking-focused technical analysis needs additional work.

Second, the variations of UAV roles in a SAGIN can lead to the extended system model for real-world scenarios. Although we focus on the discussion on the aerial BS role of UAVs, they can also be modeled as a relay node [80]. In addition, the consideration of variable speed and altitude keeping schemes, and complex cooperative schemes for state updates require further exploration.

Third, setting the objective functions and constraints in the algorithms for supporting additional application-specific scenarios is another challenge. We have considered as many factors as possible to mimic a real-world scenario. However, some unexpected situations may still exist, such as weather and environmental conditions affecting link conditions, which can be hard to predict and be mathematically modelled. This still requires future work.

Last but not least, the algorithmic variations based on the algorithms we presented in this paper may be employed to improve the performance metrics further. For example, a DRL method [81] may be used to handle dynamics and scalable problems efficiently. Deep Q-learning algorithms can be used to solve state-space explosions and improve efficiency for a complex optimization problem. On the other hand, PSO has recently been adopted in ensemble methods for the ML algorithms, such as neural networks, for hyper-parameter tuning. It has also been used as a heuristic search scheme for RL algorithms. Another future direction can be the combined use of PSO and RL together to deal with more dynamic scenarios arising from our formulated problem.

IX. CONCLUSION

Integrating UAVs into space networks and TNs faces many challenges in terms of complexity, scalability and flexibility requirements for the next-generation telecommunications networks. Although a UAV-assisted SAGIN is promising to fit into various scenarios, deployment considerations are often viewed as a barrier for real-life applications. This paper has

reviewed the recent algorithmic approaches in RL, satisfaction-based learning, and heuristic approaches. We provide key technical comparisons between these approaches in real-world scenarios. Our evaluation results have provided the simulation results to compare the performance metrics among the representative algorithms in these approaches. The simulation results reveal that the satisfaction algorithm combined with channel allocation outperforms other algorithms. With fair, consistent, and technical comparisons, our work can be used to guide the future design of UAV-assisted SAGIN missions and systems, including the SAGIN-based Internet of Things applications.

ACKNOWLEDGMENT

The work was supported by the High-Throughput and Secure Networks Challenge Program at the National Research Council of Canada under Grant No. CH-HTSN-418.

REFERENCES

- [1] X. Lin, S. Rommer, S. Euler, E. A. Yavuz, and R. S. Karlsson, "5g from space: An overview of 3gpp non-terrestrial networks," *IEEE Communications Standards Magazine*, vol. 5, no. 4, pp. 147–153, 2021.
- [2] Y. Sun, Z. Ding, and X. Dai, "A user-centric cooperative scheme for uav-assisted wireless networks in malfunction areas," *IEEE Transactions on Communications*, vol. 67, no. 12, pp. 8786–8800, 2019.
- [3] X. Zhong, Y. Guo, N. Li, Y. Chen, and S. Li, "Deployment optimization of uav relay for malfunctioning base station: Model-free approaches," *IEEE Transactions on Vehicular Technology*, vol. 68, no. 12, pp. 11971–11984, 2019.
- [4] A. H. Arani, P. Hu, and Y. Zhu, "Fairness-aware link optimization for space-terrestrial integrated networks: A reinforcement learning framework," *IEEE Access*, vol. 9, pp. 77624–77636, 2021.
- [5] A. H. Arani, M. Mahdi Azari, W. Melek, and S. Safavi-Naeini, "Learning in the sky: Towards efficient 3D placement of UAVs," in *2020 IEEE 31st Annual International Symposium on Personal, Indoor and Mobile Radio Communications*, 2020, pp. 1–7.
- [6] A. H. Arani, M. M. Azari, P. Hu, Y. Zhu, H. Yanikomeroglu, and S. Safavi-Naeini, "Reinforcement learning for energy-efficient trajectory design of UAVs," *IEEE Internet Things J.*, pp. 1–1, 2021.
- [7] B. Fan, L. Jiang, Y. Chen, Y. Zhang, and Y. Wu, "Uav assisted traffic offloading in air ground integrated networks with mixed user traffic," *IEEE Transactions on Intelligent Transportation Systems*, pp. 1–11, 2021.
- [8] Z. Liao, Y. Ma, J. Huang, J. Wang, and J. Wang, "Hotspot: A uav-assisted dynamic mobility-aware offloading for mobile-edge computing in 3-d space," *IEEE Internet of Things Journal*, vol. 8, no. 13, pp. 10940–10952, 2021.
- [9] N. C. Luong, D. T. Hoang, S. Gong, D. Niyato, P. Wang, Y.-C. Liang, and D. I. Kim, "Applications of Deep Reinforcement Learning in Communications and Networking: A Survey," *IEEE Communications Surveys & Tutorials*, vol. 21, no. 4, pp. 3133–3174, 2019. [Online]. Available: <https://ieeexplore.ieee.org/document/8714026/>
- [10] S. Zhang, D. Zhu, and Y. Wang, "A survey on space-aerial-terrestrial integrated 5g networks," vol. 174, p. 107212. [Online]. Available: <https://www.sciencedirect.com/science/article/pii/S1389128619314045>
- [11] J. Liu, Y. Shi, Z. M. Fadlullah, and N. Kato, "Space-air-ground integrated network: A survey," *IEEE Communications Surveys Tutorials*, vol. 20, no. 4, pp. 2714–2741, 2018.
- [12] M. M. Azari, F. Rosas, K. Chen, and S. Pollin, "Ultra reliable UAV communication using altitude and cooperation diversity," *IEEE Trans. Commun.*, vol. 66, no. 1, pp. 330–344, 2018.
- [13] J. Lyu, Y. Zeng, R. Zhang, and T. J. Lim, "Placement optimization of UAV-mounted mobile base stations," *IEEE Communications Letters*, vol. 21, no. 3, pp. 604–607, 2017.
- [14] Q. Wu, Y. Zeng, and R. Zhang, "Joint trajectory and communication design for multi-UAV enabled wireless networks," *IEEE Transactions on Wireless Communications*, vol. 17, no. 3, pp. 2109–2121, 2018.
- [15] X. Jiang, Z. Wu, Z. Yin, W. Yang, and Z. Yang, "Trajectory and communication design for UAV-relayed wireless networks," *IEEE Wireless Communications Letters*, vol. 8, no. 6, pp. 1600–1603, 2019.
- [16] W. Wang, N. Zhao, L. Chen, X. Liu, Y. Chen, and D. Niyato, "UAV-assisted time-efficient data collection via uplink NOMA," *IEEE Transactions on Communications*, vol. 69, no. 11, pp. 7851–7863, 2021.
- [17] F. Cui, Y. Cai, Z. Qin, M. Zhao, and G. Y. Li, "Multiple access for mobile-UAV enabled networks: Joint trajectory design and resource allocation," *IEEE Transactions on Communications*, vol. 67, no. 7, pp. 4980–4994, 2019.
- [18] X. Jiang, Z. Wu, Z. Yin, Z. Yang, and N. Zhao, "Power consumption minimization of uav relay in noma networks," *IEEE Wireless Communications Letters*, vol. 9, no. 5, pp. 666–670, 2020.
- [19] M. D. Nguyen, T. M. Ho, L. B. Le, and A. Girard, "UAV placement and bandwidth allocation for UAV based wireless networks," in *2019 IEEE Global Communications Conference (GLOBECOM)*, 2019, pp. 1–6.
- [20] B. Shang, Y. Yi, and L. Liu, "Computing over space-air-ground integrated networks: Challenges and opportunities," *IEEE Network*, vol. 35, no. 4, pp. 302–309, 2021.
- [21] A. Baltaci, E. Dinc, M. Ozger, A. Alabbasi, C. Cavdar, and D. Schupke, "A survey of wireless networks for future aerial communications (fa-com)," *IEEE Communications Surveys Tutorials*, vol. 23, no. 4, pp. 2833–2884, 2021.
- [22] J. Lyu, Y. Zeng, R. Zhang, and T. J. Lim, "Placement optimization of uav-mounted mobile base stations," *IEEE Communications Letters*, vol. 21, no. 3, pp. 604–607, 2017.
- [23] S. Wan, J. Lu, P. Fan, and K. B. Letaief, "Toward big data processing in iot: Path planning and resource management of uav base stations in mobile-edge computing system," *IEEE Internet of Things Journal*, vol. 7, no. 7, pp. 5995–6009, 2020.
- [24] C. Zhou, W. Wu, H. He, P. Yang, F. Lyu, N. Cheng, and X. Shen, "Delay-aware iot task scheduling in space-air-ground integrated network," in *2019 IEEE Global Communications Conference (GLOBECOM)*, 2019, pp. 1–6.
- [25] F. Tang, H. Hofner, N. Kato, K. Kaneko, Y. Yamashita, and M. Hangai, "A deep reinforcement learning-based dynamic traffic offloading in space-air-ground integrated networks (sagin)," *IEEE Journal on Selected Areas in Communications*, vol. 40, no. 1, pp. 276–289, 2022.
- [26] J.-J. Shin and H. Bang, "UAV Path Planning under Dynamic Threats Using an Improved PSO Algorithm," *International Journal of Aerospace Engineering*, vol. 2020, p. 8820284, 2020. [Online]. Available: <https://doi.org/10.1155/2020/8820284>
- [27] C.-Q. Dai, X. Li, and Q. Chen, "Intelligent coordinated task scheduling in space-air-ground integrated network," in *2019 11th International Conference on Wireless Communications and Signal Processing (WCSP)*, 2019, pp. 1–6.
- [28] E. Kalantari, H. Yanikomeroglu, and A. Yongacoglu, "On the number and 3d placement of drone base stations in wireless cellular networks," in *2016 IEEE 84th Vehicular Technology Conference (VTC-Fall)*, 2016, pp. 1–6.
- [29] Z. Yuheng, Z. Liyan, and L. Chunpeng, "3-D deployment optimization of UAVs based on particle swarm algorithm," in *2019 IEEE 19th International Conference on Communication Technology (ICCT)*, 2019, pp. 954–957.
- [30] L. P. Kaelbling, M. L. Littman, and A. W. Moore, "Reinforcement learning: A survey," *Journal of artificial intelligence research*, vol. 4, pp. 237–285, 1996.
- [31] R. S. Sutton and A. G. Barto, *Reinforcement learning: An introduction*. MIT press, 1998, vol. 9, no. 5.
- [32] M. L. Puterman, *Markov decision processes: discrete stochastic dynamic programming*. John Wiley & Sons, 2014.
- [33] C. J. Watkins and P. Dayan, "Q-learning," *Machine learning*, vol. 8, no. 3, pp. 279–292, 1992.
- [34] B. Khamidehi and E. S. Sousa, "Reinforcement learning-based trajectory design for the aerial base stations," in *IEEE 30th Annual International Symposium on Personal, Indoor and Mobile Radio Communications (PIMRC)*, 2019, pp. 1–6.
- [35] H. Bayerlein, P. De Kerret, and D. Gesbert, "Trajectory optimization for autonomous flying base station via reinforcement learning," in *IEEE 19th International Workshop on Signal Processing Advances in Wireless Communications (SPAWC)*, 2018, pp. 1–5.
- [36] X. Liu, Y. Liu, Y. Chen, and L. Hanzo, "Trajectory design and power control for multi-UAV assisted wireless networks: A machine learning approach," *IEEE Trans. Veh. Technol.*, vol. 68, no. 8, pp. 7957–7969, 2019.
- [37] X. Liu, Y. Liu, and Y. Chen, "Reinforcement learning in multiple-UAV Networks: Deployment and movement design," *IEEE Trans. Veh. Technol.*, vol. 68, no. 8, pp. 8036–8049, 2019.

- [38] J. Cui, Y. Liu, and A. Nallanathan, "Multi-agent reinforcement learning-based resource allocation for UAV networks," *IEEE Trans. Wireless Commun.*, vol. 19, no. 2, pp. 729–743, 2020.
- [39] X. Liu, M. Chen, and C. Yin, "Optimized trajectory design in UAV based cellular networks for 3D users: A double Q-learning approach," *Journal of Communications and Information Networks*, vol. 4, no. 1, pp. 24–32, 2019.
- [40] M. N. Katehakis and A. F. Veinott Jr, "The multi-armed bandit problem: decomposition and computation," *Mathematics of Operations Research*, vol. 12, no. 2, pp. 262–268, 1987.
- [41] S. Ali, A. Ferdowsi, W. Saad, and N. Rajatheva, "Sleeping multi-armed bandits for fast uplink grant allocation in machine type communications," in *2018 IEEE Globecom Workshops (GC Wkshps)*, 2018, pp. 1–6.
- [42] A. H. Arani, P. Hu, and Y. Zhu, "Re-envisioning space-air-ground integrated networks: Reinforcement learning for link optimization," in *2021 IEEE Int. Conf. Commun. (ICC)*, 2021, pp. 1–6.
- [43] Y. Lin, T. Wang, and S. Wang, "Uav-assisted emergency communications: An extended multi-armed bandit perspective," *IEEE Communications Letters*, vol. 23, no. 5, pp. 938–941, 2019.
- [44] Q. Qiu, H. Li, H. Zhang, and J. Luo, "Bandit based dynamic spectrum anti-jamming strategy in software defined UAV swarm network," in *2020 IEEE 11th International Conference on Software Engineering and Service Science (ICSESS)*, 2020, pp. 184–188.
- [45] B. Wu, T. Chen, and X. Wang, "A combinatorial bandit approach to UAV-aided edge computing," in *2020 54th Asilomar Conference on Signals, Systems, and Computers*, 2020, pp. 304–308.
- [46] J. Zhu, X. Huang, Y. Tang, and Z. Shao, "Learning-aided online task offloading for UAVs-aided IoT systems," in *2019 IEEE 90th Vehicular Technology Conference (VTC2019-Fall)*, 2019, pp. 1–5.
- [47] S. K. Mahmud, Y. Liu, Y. Chen, and K. K. Chai, "Adaptive reinforcement learning framework for NOMA-UAV networks," *IEEE Communications Letters*, vol. 25, no. 9, pp. 2943–2947, 2021.
- [48] A. Fotouhi, M. Ding, L. Galati Giordano, M. Hassan, J. Li, and Z. Lin, "Joint optimization of access and backhaul links for UAVs based on reinforcement learning," in *2019 IEEE Globecom Workshops (GC Wkshps)*, 2019, pp. 1–6.
- [49] Y. Hu, M. Chen, and W. Saad, "Joint access and backhaul resource management in satellite-drone networks: A competitive market approach," *IEEE Trans. Wireless Commun.*, vol. 19, no. 6, pp. 3908–3923, 2020.
- [50] P. Mach, Z. Becvar, and M. Najla, "Joint association, transmission power allocation and positioning of flying base stations considering limited backhaul," in *2020 IEEE 92nd Vehicular Technology Conference (VTC2020-Fall)*, 2020, pp. 1–7.
- [51] Y. Gao, L. Xiao, F. Wu, D. Yang, and Z. Sun, "Cellular-connected UAV trajectory design with connectivity constraint: A deep reinforcement learning approach," *IEEE Transactions on Green Communications and Networking*, vol. 5, no. 3, pp. 1369–1380, 2021.
- [52] V. Mnih, K. Kavukcuoglu, D. Silver, A. A. Rusu, J. Veness, M. G. Bellemare, A. Graves, M. Riedmiller, A. K. Fidjeland, G. Ostrovski et al., "Human-level control through deep reinforcement learning," *nature*, vol. 518, no. 7540, pp. 529–533, 2015.
- [53] S. Zhou, B. Li, C. Ding, L. Lu, and C. Ding, "An efficient deep reinforcement learning framework for uavs," in *2020 21st International Symposium on Quality Electronic Design (ISQED)*, 2020, pp. 323–328.
- [54] A. Feriani and E. Hossain, "Single and multi-agent deep reinforcement learning for ai-enabled wireless networks: A tutorial," *IEEE Communications Surveys & Tutorials*, vol. 23, no. 2, pp. 1226–1252, 2021.
- [55] M. A. Abd-Elmagid, A. Ferdowsi, H. S. Dhillon, and W. Saad, "Deep reinforcement learning for minimizing age-of-information in UAV-assisted networks," in *2019 IEEE Global Communications Conference (GLOBECOM)*, 2019, pp. 1–6.
- [56] F. Tang, H. Hofner, N. Kato, K. Kaneko, Y. Yamashita, and M. Hangai, "A deep reinforcement learning-based dynamic traffic offloading in space-air-ground integrated networks (SAGIN)," *IEEE Journal on Selected Areas in Communications*, vol. 40, no. 1, pp. 276–289, 2022.
- [57] L. Wang, K. Wang, C. Pan, X. Chen, and N. Aslam, "Deep q-network based dynamic trajectory design for UAV-aided emergency communications," *Journal of Communications and Information Networks*, vol. 5, no. 4, pp. 393–402, 2020.
- [58] Q. Liu, L. Shi, L. Sun, J. Li, M. Ding, and F. Shu, "Path planning for UAV-mounted mobile edge computing with deep reinforcement learning," *IEEE Transactions on Vehicular Technology*, vol. 69, no. 5, pp. 5723–5728, 2020.
- [59] F. Tang, Y. Zhou, and N. Kato, "Deep reinforcement learning for dynamic uplink/downlink resource allocation in high mobility 5G HetNet," *IEEE Journal on Selected Areas in Communications*, vol. 38, no. 12, pp. 2773–2782, 2020.
- [60] P. Luong, F. Gagnon, L.-N. Tran, and F. Labeau, "Deep reinforcement learning-based resource allocation in cooperative UAV-assisted wireless networks," *IEEE Transactions on Wireless Communications*, vol. 20, no. 11, pp. 7610–7625, 2021.
- [61] J. Tang, J. Song, J. Ou, J. Luo, X. Zhang, and K.-K. Wong, "Minimum throughput maximization for multi-UAV enabled WPCN: A deep reinforcement learning method," *IEEE Access*, vol. 8, pp. 9124–9132, 2020.
- [62] S. Ross and B. Chaib-draa, "Satisfaction equilibrium: Achieving cooperation in incomplete information games," in *Conference of the Canadian Society for Computational Studies of Intelligence*. Springer, 2006, pp. 61–72.
- [63] S. M. Perlaza, H. Tembine, S. Lasaulce, and M. Debbah, "Satisfaction equilibrium: A general framework for QoS provisioning in self-configuring networks," in *2010 IEEE Global Telecommunications Conference GLOBECOM 2010*, 2010, pp. 1–5.
- [64] —, "Quality-of-service provisioning in decentralized networks: A satisfaction equilibrium approach," *IEEE J Sel Top Signal Process*, vol. 6, no. 2, pp. 104–116, 2012.
- [65] M. Simsek, M. Bennis, and I. Guvenc, "Context-aware mobility management in hetnets: A reinforcement learning approach," in *2015 IEEE WCNC*, 2015, pp. 1536–1541.
- [66] B. Ellingsæter, "Frequency allocation game in satisfaction form," *Transactions on Emerging Telecommunications Technologies*, vol. 25, no. 12, pp. 1238–1251, 2014.
- [67] A. H. Arani, A. Mehdodniya, M. J. Omid, and M. F. Flanagan, "Satisfaction based channel allocation scheme for self-organization in heterogeneous networks," in *2018 IEEE Global Communications Conference (GLOBECOM)*, 2018, pp. 1–6.
- [68] S. M. Perlaza, H. Tembine, S. Lasaulce, and M. Debbah, "Satisfaction equilibrium: A general framework for QoS provisioning in self-configuring networks," in *IEEE GLOBECOM 2010*, 2010, pp. 1–5.
- [69] A. Hajijamali Arani, M. J. Omid, A. Mehdodniya, and F. Adachi, "Minimizing base stations' on/off switchings in self-organizing heterogeneous networks: A distributed satisfactory framework," *IEEE Access*, vol. 5, pp. 26 267–26 278, 2017.
- [70] A. H. Arani, M. J. Omid, A. Mehdodniya, and F. Adachi, "A distributed satisfactory sleep mode scheme for self-organizing heterogeneous networks," in *Electrical Engineering (ICEE), Iranian Conference on*, 2018, pp. 476–481.
- [71] J. Kennedy and R. Eberhart, "Particle swarm optimization," in *Proceedings of ICNN'95-international conference on neural networks*, vol. 4. IEEE, 1995, pp. 1942–1948.
- [72] H. J. Na and S.-J. Yoo, "Pso-based dynamic UAV positioning algorithm for sensing information acquisition in wireless sensor networks," *IEEE Access*, vol. 7, pp. 77 499–77 513, 2019.
- [73] J. Plachy, Z. Becvar, P. Mach, R. Marik, and M. Vondra, "Joint positioning of flying base stations and association of users: Evolutionary-based approach," *IEEE Access*, vol. 7, pp. 11 454–11 463, 2019.
- [74] Y. Cheng, Y. Liao, and X. Zhai, "Energy-efficient resource allocation for UAV-empowered mobile edge computing system," in *2020 IEEE/ACM 13th International Conference on Utility and Cloud Computing (UCC)*, 2020, pp. 408–413.
- [75] A. H. Arani, A. Mehdodniya, M. J. Omid, F. Adachi, W. Saad, and I. Guvenc, "Distributed learning for energy-efficient resource management in self-organizing heterogeneous networks," *IEEE Trans. Veh. Technol.*, vol. 66, no. 10, pp. 9287–9303, 2017.
- [76] R. K. Jain, D.-M. W. Chiu, W. R. Hawe et al., "A quantitative measure of fairness and discrimination," *Eastern Research Laboratory, Digital Equipment Corporation, Hudson, MA*, 1984.
- [77] M. R. Akdeniz, Y. Liu, M. K. Samimi, S. Sun, S. Rangan, T. S. Rappaport, and E. Erkip, "Millimeter wave channel modeling and cellular capacity evaluation," *IEEE J. Sel. Areas Commun.*, vol. 32, no. 6, pp. 1164–1179, 2014.
- [78] G. Fontanesi, A. Zhu, and H. Ahmadi, "Outage analysis for millimeter-wave fronthaul link of UAV-aided wireless networks," *IEEE Access*, vol. 8, pp. 111 693–111 706, 2020.
- [79] L. Sun, X. Song, and T. Chen, "An Improved Convergence Particle Swarm Optimization Algorithm with Random Sampling of Control Parameters," *Journal of Control Science and Engineering*, vol. 2019, p. 7478498, 2019. [Online]. Available: <https://doi.org/10.1155/2019/7478498>
- [80] M. Gapeyenko, V. Petrov, D. Moltchanov, S.-P. Yeh, N. Himayat, and S. Andreev, "Comparing capacity gains of static and uav-based

millimeter-wave relays in clustered deployments,” in *2020 IEEE International Conference on Communications Workshops (ICC Workshops)*, 2020, pp. 1–7.

- [81] V. Mnih, K. Kavukcuoglu, D. Silver, A. A. Rusu, J. Veness, M. G. Bellemare, A. Graves, M. Riedmiller, A. K. Fidjeland, G. Ostrovski, S. Petersen, C. Beattie, A. Sadik, I. Antonoglou, H. King, D. Kumaran, D. Wierstra, S. Legg, and D. Hassabis, “Human-level control through deep reinforcement learning,” *Nature*, vol. 518, no. 7540, pp. 529–533, 2015. [Online]. Available: <https://doi.org/10.1038/nature14236>